A Self-Noise Model for the German DEPAS OBS Pool

by Simon C. Stähler, Mechita C. Schmidt-Aursch, Gerrit Hein, and Robert Mars

ABSTRACT

Ocean-bottom seismometers (OBSs) allow us to extend seismological research to the oceans to constrain offshore seismicity but also image the marine subsurface. A challenge is the high noise level on OBS records, which is created not only by bottom currents but also by the specific seismometer models used. We present a quantitative noise model for the LOBSTER OBS, which is the main instrument of the DEutscher Geräte-Pool für Amphibische Seismologie (DEPAS), currently the largest European OBS pool, stationed at AWI Bremerhaven. Studying sensor noise in vault conditions and current sensitivity at an oceanographic measurement mast, we can show that the previously reported high noise level of the instrument is caused by the original sensor (Güralp CMG-40T-OBS). We also show that a strong signal that has been reported between 1 and 5 Hz can be attributed to head-buoy cable strumming. We provide a current-dependent quantitative noise model that can be used for experiment design in future deployments and show that the performance of the pool OBS can be improved at moderate cost by replacing the CMG-40T-OBS with a sensor of a proven noise floor below 10^{-8} nm/s^2, for example, a Trillium compact.

INTRODUCTION

The DEutscher Geräte-Pool für Amphibische Seismologie (DEPAS) pool (Alfred-Wegener-Institut Helmholtz-Zentrum für Polar- und Meeresforschung *et al.*, 2017) is currently the largest pool of wideband ocean-bottom seismometers (OBSs) in Europe. It consists of 80 LOBSTER OBS, manufactured by K.U.M., which are equipped with Güralp CMG-40T-OBS sensors. Apart from DEPAS, the LOBSTER is also part of the OBS pools of the Royal Observatory of the Spanish Navy, the German Bundesanstalt für Geowissenschaften und Rohstoffe (BGR), Geomar in Kiel, the Danish seismometer pool DanSeis, and the University of Lisbon. The LOBSTER is a titanium frame around several buoyancy bodies of syntactic foam, with the seismic sensor, the data acquisition unit, and the batteries stored in titanium tubes (see Fig. 1). The seismometer is fixed within the frame and pressed against the steel anchor.

This design choice makes the whole OBS easy to transport and deploy. At the same time, this increases current-induced long-period tilt noise because the OBS frame has a larger cross section than a smaller external seismometer package (Webb, 1998). This has become an issue in the RHUM-RUM experiment (Barruol and Sigloch, 2013), in which 47 of the DEPAS instruments were deployed around La Réunion in the southwestern Indian Ocean: Even in relatively quiet regions, the noise level exceeded the new high-noise model (Peterson, 1993) at a period of 20 s (Stähler *et al.*, 2016, their fig. C2). In the same experiment, French LCPO-2000 OBS equipped with a Trillium 240 sensor and installed at comparable locations recorded a 40-dB lower noise level in the period range between 40 and 100 s, which shows that this signal was not of tectonic or oceanic origin. An explanation for the difference could be tilt noise from ocean-bottom currents because the LCPO-2000 has the seismometer in a separate sphere next to the OBS frame. As has been discussed by Stähler *et al.* (2016), on the vertical component, the high noise beyond 10 s is essentially constant on the LOBSTERs over the whole duration of the experiment, which is inconsistent with time-varying currents as a source. The French stations show strong temporal variability in long-period noise on all components but tens of decibels below the LOBSTER level. Apart from the OBS shape, the main difference is the sensor because the Trillium 240 is a true broadband instrument, albeit with a much higher mass and power consumption than the CMG-40T-OBS. Other users of the DEPAS pool (e.g., Dewangan *et al.*, 2017) confirmed this observation. Even though instruments of the pool have been used in roughly 40 passive and active experiments so far (e.g., Meier *et al.*, 2007; Geissler *et al.*, 2010; Barruol and Sigloch, 2013; Geissler and Schmidt, 2013), the self-noise of this OBS package has not been systematically examined yet to separate effects of OBS frame and sensor. Because the OBS pool is being used increasingly more often by terrestrial seismologists without specific knowledge or interest in the peculiarities of ocean-bottom seismology, a quantitative self-noise model of the instrument is highly relevant for planning future experiments with the pool. To this end and to test whether the LOBSTER design is fundamentally compatible with broadband seismology, we conducted an examination of the seismic sensor itself under vault conditions (see Sensor Self-Noise section), the influence of currents on the OBS frame (see Tilt section), and the head-buoy cable, which is another potential noise source in the LOBSTER design (see the Head-Buoy Strumming section).

doi: 10.1785/0220180056

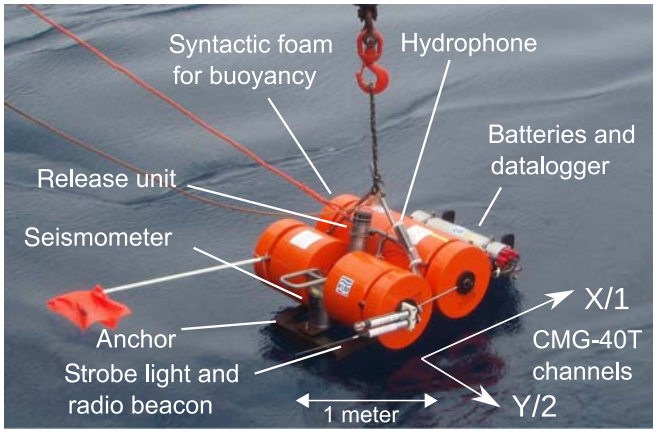

▲ **Figure 1.** A LOBSTER-type instrument from the German DEutscher Geräte-Pool für Amphibische Seismologie (DEPAS) pool before deployment. The seismic sensor is fitted in a vertical titanium pressure cylinder between two syntactic foam buoys and wedged against the steel anchor beneath it. Two horizontal titanium cylinders in the background contain the data recorder and alkaline or lithium batteries. The broadband hydrophone (corner period 100 s) is strapped to the A-shaped titanium frame that protrudes from the center of the buoy assemblage. Whereas the channel orientation of the CMG-40T-OBS is fixed with respect to the frame, the orientation of a Trillium compact may change during leveling. Adapted with permission from Stähler *et al.* (2016).

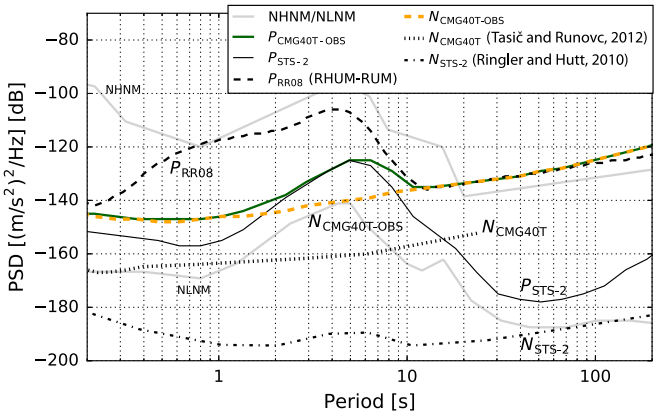

▲ **Figure 2.** Median power spectral density of vertical ambient noise measured in a seven-day period at Conrad observatory of a CMG-40T-OBS ($P_{CMG-40T-OBS}$, gray solid line) and a collocated STS-2 (P_{STS-2}, black line) and derived from it the self-noise ($N_{CMG-40T-OBS}$, thick gray dashed line). For comparison, the self-noise of the land version of a 30-s CMG-40T ($N_{CMG-40T}$, Tasič and Runovc, 2012, dotted) and the STS-2 (N_{STS-2}, Ringler and Hutt, 2010, dashed–dotted) is plotted. The new noise model explains the noise observed by the RHUM-RUM project beyond 10-s period (station YV.RR08, P_{RR08}). The thin gray lines show the low- and high-noise models of Peterson (1993; new low-noise model [NLNM] and new high-noise model [NHNM]).

SENSOR SELF-NOISE

The LOBSTER OBS was initially sold with an OBS-specific version of the Güralp CMG-40T. This sensor, advertised as a robust broadband analog seismometer, has been used by observatories and seismic services, mainly for temporary deployments, for decades. Its original version had a flat response to an upper corner period of 10 s, but it was widely sold in versions with corner periods of 30, 60, and 120 s. The self-noise exceeds the new low-noise model (NLNM; Peterson, 1993) for periods of more than 10 s (Tasič and Runovc, 2012), which puts the instrument into the wideband or intermediate class. Although this noise is relatively high compared with more recent instruments of similar size, such as the Trillium compact (Ringler and Hutt, 2010), it is possible to record teleseismic events of magnitude 5 and above in a quiet setting at periods of 30 s and less.

The DEPAS pool uses the 60-s instrument in a version that was modified by Güralp for OBS usage by reducing power consumption and adding a mechanical gimbal system for automated leveling. The sensor was placed in a titanium casing manufactured by K.U.M. These modifications seem to have a profound effect on instrument self-noise. The modified version is referred to as CMG-40T-OBS throughout the article.

To determine the self-noise of the CMG-40T-OBS, two sensors in the titanium pressure tube were installed for two weeks at the Conrad observatory of the Central Institute for Meteorology and Geodynamics (ZAMG) in Austria. The data logger was the same SEND-MCS that is used in the LOBSTER.

To determine a quantitative self-noise model, the measurement of seven quiet days, recorded after two days of settling, was compared with the noise record of a collocated STS-2 seismometer (International Federation of Digital Seismograph Networks [FDSN] ID: OE.CONA.51.BHZ). Details of determining an instrument self-noise using one or two reference sensors can be found in Ringler *et al.* (2014), but given that the self-noise of the CMG-40T-OBS is orders of magnitude higher than the one of an STS-2, we used the simple method of Holcomb (1989) to calculate a self-noise curve (see Fig. 2 and Table 1). The power spectral density was calculated using Welch's method, with a time window of 2 hrs, overlapping by 1 hr. The obtained self-noise consistently exceeds by 20 dB, the self-noise determined by Tasič and Runovc (2012) for the land version of the CMG-40T. Table 1 presents a smoothed version of our self-noise estimate. It exceeds the NLNM at all periods and the NHNM at periods longer than 20 s. The recorded noise floor is extremely similar on all components of the two instruments and equal to the one on the vertical component of the RHUM-RUM installations (see Fig. 3, left column). This confirms that the excessive long-period noise on the vertical component of the first LOBSTER generation is not caused by sea-floor currents but rather by the sensor itself.

FRAME NOISE

Tilt

Seismometers are susceptible to tilt, which causes a redistribution of gravitational force between the horizontal and vertical

Table 1
Median Instrument Self-Noise Model for the CMG-40T-OBS Determined from Vault Measurements at Conrad Observatory

Period (s)	Median Self-Noise (dB) ($(m/s^2)^2/Hz$)
0.20	−144
0.36	−147
0.78	−147
4.25	−140
30	−132
50	−130
200	−120
300	−114

components. The effect on OBSs has been described in detail by Crawford and Webb (2000). The LOBSTER OBS type has its seismometer installed into the frame, which makes the instrument more susceptible to currents. Because the large cross-section area of the OBS frame means that currents will shake it more than a separate, smaller sensor housing, sensor tilt is increased. Therefore, integration into the frame is generally discouraged by long-period seismologists. On the other hand, it greatly facilitates handling of the unit, especially in surveys with a large number of instruments, which is why it has been used for the LOBSTER design. Whereas the RHUM-RUM data showed no clear sign of tilt on the vertical component of most DEPAS stations (an exception may be RR44, installed in a rugged region of a mid-ocean ridge, which may have experienced stronger currents, see Stähler *et al.* [2015]), the National Institute for Earth Sciences and Astronomy (INSU) broadband seismometers showed tilt. This suggests that tilt noise on the vertical component does not exceed self-noise of the CMG-40T-OBS for typical bottom current velocities.

To test this hypothesis, we installed two LOBSTER packages next to an oceanographic measurement mast with a permanently installed doppler current profiler. The location is the Darss Sill, a threshold in the southwestern Baltic Sea (Lemke *et al.*, 1994), which regularly experiences bottom currents of up to 1 m/s during major saltwater inflow events (Mohrholz *et al.*, 2015). The mast is maintained by the Leibniz Institute for Baltic Sea Research (IOW) in Rostock. It measures wind speed, wave height, period and direction, and current and water profiles with a temporal resolution of one hour at least (Krüger, 2000). For the time of the experiment, we converted the data to miniSEED format. It has been assigned FDSN station code 6H.DARS0.

For the test installation, one LOBSTER was equipped with the classic CMG-40T-OBS (6H.DARS1) and the other with a Trillium compact (6H.DARS2). The instruments were otherwise identical, and both used the SEND-MCS data logger. The OBS was separated by 120 m, in a water depth of 21.6 m, on a flat, sandy ocean bed between 30 January 2016 and 2 April 2016. Figure 3 shows probabilistic power spectral densities (PPSDs, following McNamara and Buland, 2004) for the 60-day installation. The PPSDs were calculated using ObsPy (Krischer *et al.*, 2015) in time windows of 1800 s with an overlap of 900 s. At this water depth, wind-generated waves have a considerable horizontal motion at the sea floor, which creates a noise signal in the period range of 3–10 s. However, long-period noise on the Güralp-equipped instrument is comparable to the deep-sea installation during RHUM-RUM. At the same time, the noise floor in the Trillium compact record goes down to the published self-noise of the instrument at around 100-s period. The Trillium compact record also shows variations over the installation period.

To test the effect of currents, we bandpassed the data between 80 and 160 s, split the seismic record into one-hour-long windows, and calculated the signal power for each window. This was converted to power spectral density by dividing by the bandwidth and binned by current velocity in the same time window. Figure 4 shows the median noise in each current bin versus current velocity 2 m above sea floor. To reduce the effect of wave-induced bottom currents, only time windows with wind speeds below 8 m/s were taken into account. The plot shows that below currents of 7–8 cm/s, the noise level shows no strong dependence of currents, but it increases roughly with fourth power of current velocity beyond 10 cm/s. The horizontal channels of both sensors show a similar behavior, in which the noise level on the Y channel is 10 dB higher compared with the X channel. The median noise levels at low currents are −110 dB and −95 dB for X and Y channel, respectively. As shown in Figure 1, the Y channel is fixed along the shorter axis of the frame, which has a lower moment of inertia than the long axis, along which X is oriented. This allows currents to tilt the frame stronger in the direction of channel Y. These noise levels seem to be an intrinsic property of the LOBSTER frame. The vertical channel of DARS2 (Trillium compact) shows an even stronger current dependency than the horizontal channels, with a baseline of −150 dB. This is close to the median self-noise of −155 dB at 120 s found by Ringler and Hutt (2010) for a Trillium compact. The noise on the vertical channel of the CMG-40T-OBS-equipped station DARS1 has a baseline of −120 dB, which is approximately the value found in the Conrad observatory (see Table 1). It only increases with power < 1 and only for currents above 12 cm/s. This confirms the assumption that the vertical noise level of the classical LOBSTER with a CMG-40T-OBS seismometer is not much influenced by currents but rather the instrument self-noise itself.

The horizontal channel orientation of the Trillium compact (DARS2) with respect to the OBS frame does not have to be the same as shown in Figure 1 because the channels can be reoriented randomly during leveling. Therefore, we measured the frame orientation with an ROV dive and the channel orientation from Rayleigh-wave polarization using the DLOPy package (Doran and Laske, 2017). Both values agreed within 5°.

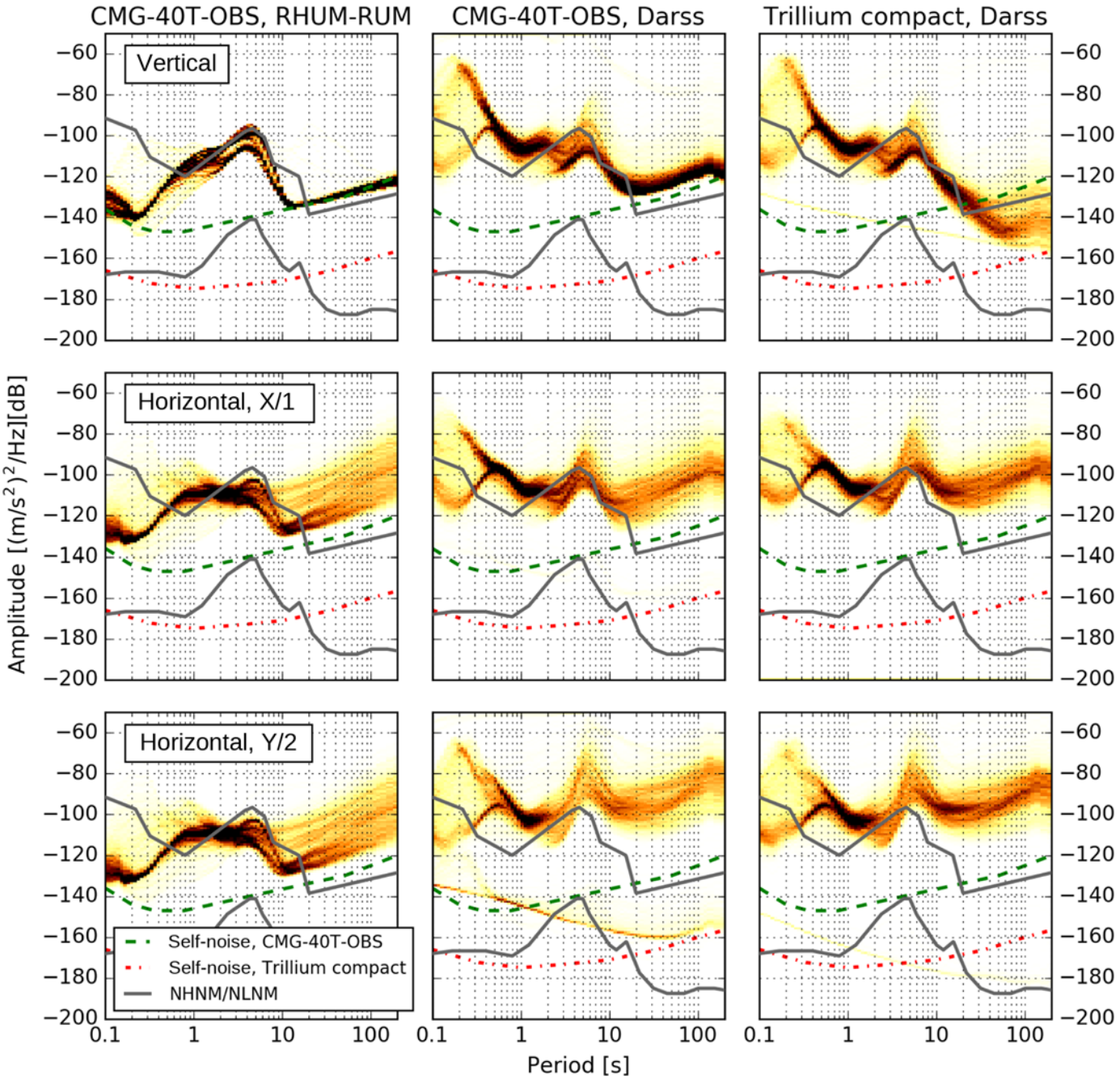

▲ **Figure 3.** Comparison of probabilistic power spectral densities (PPSDs) obtained at the RHUM-RUM experiment (channels 21 YV.RR08.00.BH?, water depth: 4190 m) with two stations at Darss Sill, (6H.DARS1.00.HH? and 6H.DARS2.00.HH?, Baltic Sea, 22 m depth). The two shallow ocean-bottom seismometers (OBSs) show a much higher general noise level due to wave-induced bottom currents around 5–10 s, but the long-period noise level is comparable for both CMG-40T-OBS-stations. The Trillium compact-equipped station has a much lower long-period noise floor in comparison, especially on the vertical axis. Darker colors correspond to higher probabilities with 8% as maximum value.

Head-Buoy Strumming

The PPSDs show diffuse signal energy between 0.1 and 1 s. As first reported by Snelling (2015, p. 31), during the RHUM-RUM experiment, this signal is harmonic, with a fundamental period of 0.4–1 s and multiple clear overtones. The author ruled out whales, icebergs, and volcanic tremor as sources of the signal due to frequency content and the fact that the signal was not observed coherently over multiple stations. Our experiment in the Baltic Sea suggests that this peak is caused by current strumming of the head-buoy cable. Mooring cables are known to be affected by strumming from currents; Karman streets in the water, which have a characteristic shedding

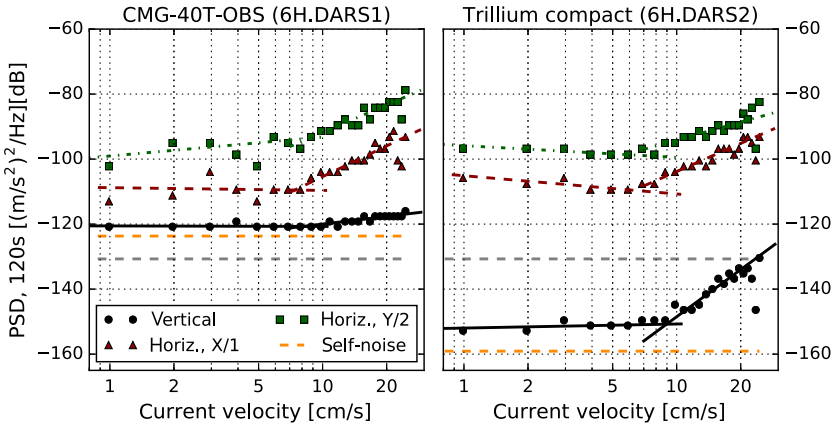

▲ **Figure 4.** Noise level of the seismometer channels of two LOBSTER versus current velocities. DARS1 was using a Güralp CMG-40T-OBS sensor and DARS2 a Trillium compact. The self-noise curve for DARS1 is the one given in Table 1; for DARS2, it is taken from Ringler and Hutt (2010). The lines are separate fits for currents below 8 cm/s and above. Ocean gravity waves cause short-period currents, which are not detected by the current detector; therefore, the noise floor at low current velocity values is higher than expected.

frequency cause oscillations of the cable. This effect is enhanced if the vortex shedding frequency is equal or close to the resonant frequency, an effect called wake or lock-in in the literature (Skop and Griffin, 1975; Griffin, 1985). The exact mechanisms for flexible cables are rather complicated and can usually be only solved numerically. (A good overview is given in Triantafyllou *et al.*, 2016.) For the simplified case of a homogeneous cable with length L and linear density λ_m, the resonance frequency $f_{\mathrm{CF},n}$ of mode n is given by Mersenne's law:

$$f_{\mathrm{CF},n} = \frac{(n+1)}{2L}\sqrt{\frac{F_{\mathrm{buoy}}}{\lambda_m}}, \tag{1}$$

in which F_{buoy} is the tension on the cable created by the buoyancy of the head buoy. The LOBSTER head-buoy cable has a linear density of $\lambda_m = 0.145$ kg/m. The buoyancy of the buoy itself is $F_{\mathrm{buoy}} = V(\rho_{\mathrm{H_2O}} - \rho_{\mathrm{foam}})g$, with $V = 0.2\ \mathrm{m} \times 0.15\ \mathrm{m} \times 0.13\ \mathrm{m} = 3.910^{-3}\ \mathrm{m}^3$ and $\rho_{\mathrm{foam}} = 640\ \mathrm{kg/m}^3$, resulting in $F_{\mathrm{buoy}} = 13.8$ N.

Generally, the cable is of length $L = 10$ m, resulting in $f_{\mathrm{CF},0} \approx 0.48$ Hz. Because the actual cable contains several knots at irregular distances, the exact value of $f_{\mathrm{CF},0}$ will probably differ (most likely less because the knots increase the mass of the rope).

The Reynolds number Re of the system at hand is

$$\mathrm{Re} = \frac{vd}{\nu}, \tag{2}$$

in which ν is the kinematic viscosity of water, $\nu(T = 4°\mathrm{C}) \approx 1.6 \times 10^{-6}\ \mathrm{m}^2/\mathrm{s}$, and the characteristic length is the diameter of the rope, $d = 0.02$ m, resulting in $\mathrm{Re} \approx 1250$ for $v = 0.1$ m/s. In this Reynolds regime, vortex streets are generated with a specific shedding frequency of

$$f_{\mathrm{vort}} = \mathrm{St} * \frac{v}{d}, \tag{3}$$

in which St is the Strouhal number, $\mathrm{St} = 0.21$. Thus, the vortex shedding frequency f_{vort} varies linearly with current velocity v as

$$f_{\mathrm{vort}} = 10.5 \cdot v\mathrm{Hz}. \tag{4}$$

For a current velocity of $v = 0.1$m/s, the vortex shedding frequency is $f_{\mathrm{vort}} = 1.05$ Hz, which is very close to the first overtone of the resonance frequency $f_{\mathrm{CF},1} = 0.976$ Hz. Because of this coincidence, resonant modes in the head-buoy cable are excited at moderate current velocities for this OBS model. The higher modes create the harmonic signal (see Fig. 6a). The resulting narrow peaks at frequencies above 1.5 Hz can be seen well in daily spectrograms of LOBSTER installations (Fig. 5). The exact frequency is strongly current dependent and a result of the lock-in. In Figure 3, these current-modulated peaks create the diffuse signal for periods of 0.1–1 s.

To reduce the strumming signal, the rope resonance frequency should be moved away from the excitation frequencies. Given the overtones, even a much longer rope would resonate with current in some way (see Fig. 6b). Therefore, the most promising solution would be to reduce the strumming efficiency, either by choosing a thinner rope or by pairing the cable.

DISCUSSION

Our experiment shows that the LOBSTER OBS design fundamentally allows passive seismology over a wide frequency range but that the original design was limited by the sensor. As an example to test the usability of the instrument package with a better sensor for long-period seismology, we looked for multiple-orbit Rayleigh waves: at 200-s period, the Trillium compact noise floor has a self-noise of 10 $\mathrm{nm/s}^2 = -160$ dB. Comparison with synthetic data, calculated with AxiSEM and Instaseis (Nissen-Meyer *et al.*, 2014; van Driel *et al.*, 2015) using the anelastic PREM model (Dziewoński and Anderson, 1981) and the record of a STS-2 broadband instrument in 50-km distance shows the expected amplitude of R5 for a magnitude 7.8 event is slightly above this. Figure 7 shows that R5 of the Nepal earthquake (25 April 2015 06:11:25) was indeed recorded on 6H.DARS2, a LOBSTER equipped with said Trillium compact, even though it was installed in adverse conditions, that is, very shallow in a high-current regime on soft soil. The collocated current sensor was not working at the time of the earthquake, but records eight hours earlier and later showed values of 0.2 m/s. This means that the rugged construction of the LOBSTER and

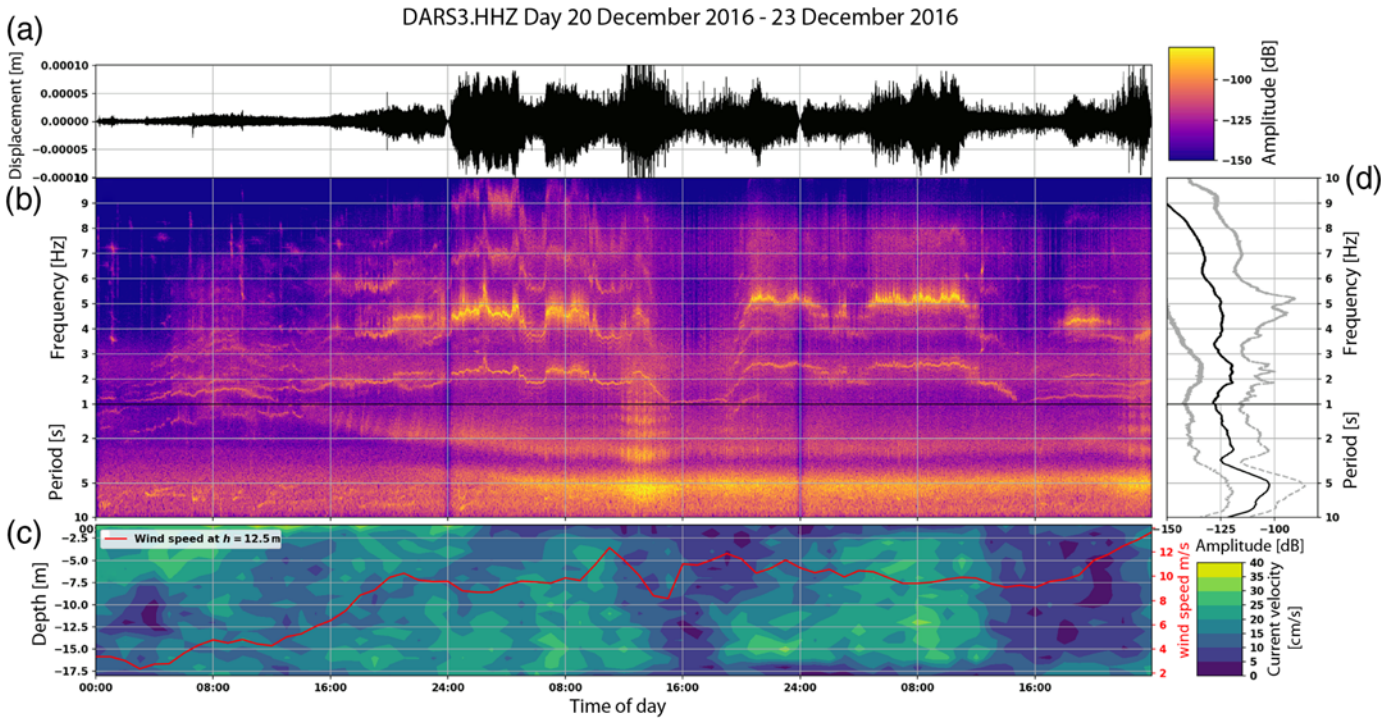

▲ **Figure 5.** Harmonic signal created by the head buoy. (a) Displacement record of 3 days, filtered between 0.1 and 10 Hz. (b) Acceleration spectrogram of the same seismic record. Below 1 Hz, the signal is dominated by local gravity waves. Above 1 Hz, a harmonic signal is clearly visible, which corresponds to the high-current time windows. (c) Oceanographic data for comparison. The red line marks the wind speed in 12.5-m altitude measured at the measurement mast. The background colors show the absolute value of current velocities in the water column. The water depth is 20 m, so the head buoy is affected by currents in water depth of more than 10 m. (d) Median (black) and 5th and 95th percentiles (gray) of spectral acceleration power.

the sensor integration into the frame do not generally prohibit broadband seismology.

On quiet days, long-period noise recorded on the horizontal component at Darss Silt is only a few decibels above the noise of a deep sea INSU OBS with a separate seismometer sphere at a period of 100 s. This shows that on the horizontal component, the effect of separating the OBS is not very high, and the extra effort at deployment and recovery must be carefully weighted.

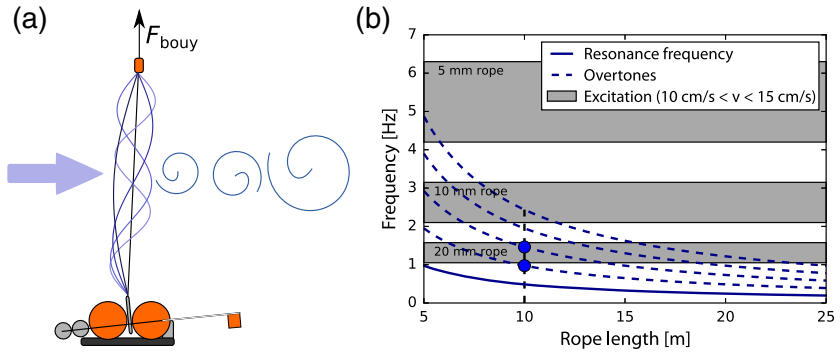

▲ **Figure 6.** (a) Excitation mechanism of the current-generated harmonic signal. (b) Resonance frequency of the head buoy mooring for different rope lengths, assuming a linear density and force described in the text. For comparison, the excitation frequencies between 10 and 15 cm/s for different rope thicknesses are shown. The current rope length of the LOBSTERs is around 10 m, and the diameter is 17–20 mm, which means that the first and second overtone are regularly excited (blue dots). The resonance frequency could be moved out of the excitation range by choosing a thinner or longer cable.

Our results also show that the OBS version of the CMG-40T sensor is not comparable in performance with the land version. The power consumption of the OBS version is reduced to 100 mW, which allows for year-long deployments with only around 200 lithium cells. These adaptations have impacted self-noise strongly. It cannot be said with last certainty whether the source of the higher self-noise is the sensor itself or the titanium casing in which it was installed by K.U.M., but testing the sensor outside the casing delivered similar self-noise levels as shown in the Sensor Self-Noise section. At the time when the DEPAS pool was designed (2005), the CMG-40T-OBS was the optimum for its role in terms of price, power consumption, size, and availability. The instrument performance was not tested independently of the manufacturer before acquisition; a lesson from this example is that this should be mandatory for such large

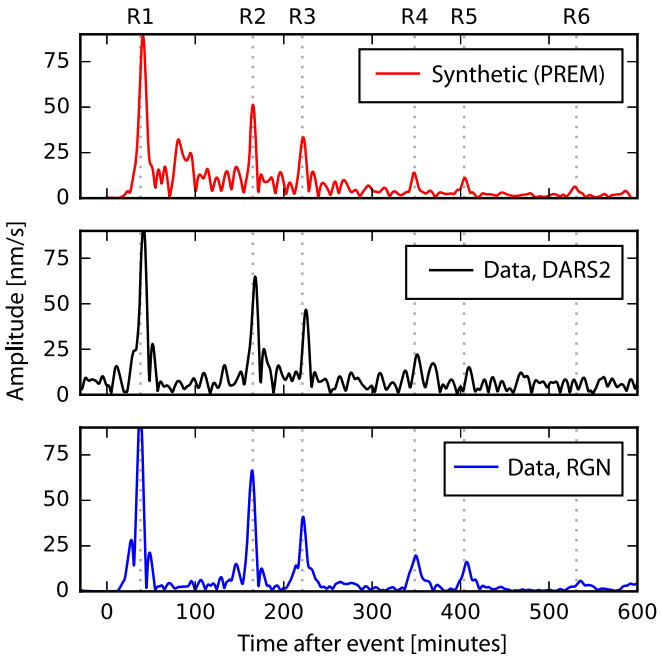

▲ **Figure 7.** Envelope of vertical ground acceleration measured after the M 7.8 earthquake in Nepal, 25 April 2015 06:11:25, filtered between 160 and 240-s period. The waveforms were recorded on a LOBSTER with a Trillium compact (DARS2) and an STS-2 broadband instrument at the station GE.RGN of the German regional network. Even though DARS2 is installed on soft soil in only 20-m water depth, multiple-orbit Rayleigh waves up to R5 are visible.

purchases of a modified instrument. Since 2005, wideband seismometers of similar size but with better performance have been designed, which allows us to improve performance of the DEPAS pool at relatively low cost. The seismometer is a quarter of the total cost of an OBS, so it will be possible to replace the CMG-40T-OBS sensors in the DEPAS pool by Trillium compacts over the next years. With the CMG-40T-OBS, the LOBSTER is suited best for regional seismicity studies and active experiments; waveform tomography is restricted to
10 stronger earthquakes (above M6.5). Ambient noise methods have been successfully applied for short interstation distances (100–200 km) (Ryberg *et al.*, 2017) but are limited to a narrow period range between 2 and 10 s, which allows imaging of the crust and uppermost mantle only.

The comparison of long-period noise and measured currents shows no clear relationship below 8 cm/s current velocity. There is no clear reason why weaker currents should tilt the OBS frame in a fundamentally different way. Our interpretation is that the noise floor for low currents is either caused by the sensor self-noise or by wave-induced water motion that is below the temporal resolution of the Doppler current profiler.

The LOBSTER frame has a meter-long flag that sits horizontally after deployment. It was suspected as a source of the harmonic signal. However, our measurements in the Baltic Sea clearly show that the harmonic signal is also excited by currents a few meters above the sea floor. Also, the horizontal flag would be excited strongest by currents orthogonal to it (Y direction in Fig. 1), but from measurements at Darss Silt, we find that the harmonic signal is almost independent of current direction relative to the OBS. To reduce the level of strumming noise, it would be necessary to modify the head-buoy cable either by decreasing its length to increase its resonance frequency or increasing the vortex shedding frequency by choosing a much thinner cable. Because the rope has an important role during retrieval of the instrument, especially under stormy conditions, both options are only possible to some extent and need to be weighted. If the design allows it, the best option is to fix the head buoy at the OBS until release from the bottom weight, which gets rid of this noise source altogether.

CONCLUSION

Our test deployments in the Baltic Sea show that the LOBSTER frame can be used for broadband seismology to periods of hundreds of seconds if it is equipped with a high-fidelity wideband sensor, such as the Trillium compact. The reported high long-period noise level is mostly an effect of the original sensor (Güralp CMG-40T-OBS), which we have shown to be only suited for short-period seismology. We could also show that the strong harmonic but temporally varying noise signal above 1 Hz is caused by strumming on the head-buoy cable.

DATA AND RESOURCES

The OBS dataset at Darss silt is hosted by the GeoForschungsZentrum (GFZ) data center in Potsdam, Germany, under International Federation of Digital Seismograph Networks (FDSN) network code 6H. The RHUM-RUM data set (http://dx.doi
11 .org/10.15778/RESIF.W2011; Barruol *et al.*, 2011) is hosted by the RESIF data center in Grenoble, France, under FDSN net-
12 work code YV. The data of station GE.RGN is part of the GEOFON network (GEOFON Data Centre, 1993). Figures were created using ObsPy (Krischer *et al.*, 2015) and matplotlib (Hunter, 2007). The information about the manufacturer K.U.M. is available at http://www.kum-kiel.de. 13

ACKNOWLEDGMENTS

The authors thank the crew of FS Elisabeth Mann-Borghese for excellent support during deployment and retrieval on cruises EMB94, EMB101, EMB138, and EMB146 and Wolfgang Roeder for the permission to record at Darss Silt. Volker Mohrholz helped in interpreting the current profiles. The Zentralanstalt für Meteorologie und Geodynamik (ZAMG) and the Network of Research Infrastructures for European Seismology (NERIES; EU-Contract Number: 026130) enabled us to conduct the test in the Conrad Observatory. This research received funding from Deutsche Forschungsgemeinschaft (DFG) Grant SI1538/2-1 RHUM-RUM. The article was improved by comments from two anonymous reviewers.

REFERENCES

14 Alfred-Wegener-Institut Helmholtz-Zentrum für Polar- und Meeresfor-
15 schungSchmidt-Aursch, M. C., and C. Haberland (2017). DEPAS (Deutscher Geräte-Pool für amphibische Seismologie): German Instrument Pool for Amphibian Seismology, *J. Large-Scale Res. Facil.* **3,** no. A122, ISSN: 2364–091X, doi: 10.17815/jlsrf-3-165.

Barruol, G., and K. Sigloch (2013). Investigating La Réunion hot spot from crust to core, *Eos Trans. AGU* **94,** no. 23, 205–207, doi: 10.1002/2013EO230002.

Barruol, G., K. Sigloch, and , and RHUM-RUM group(2011). *RHUM-RUM experiment, 2011-2015, code YV (Réunion Hotspot and Upper Mantle - Réunion's Unterer Mantel) funded by ANR, DFG, CNRS-INSU, IPEV, TAAF, instrumented by DEPAS, INSU-OBS, AWI and the Universities of Muenster*, Bonn, La Réunion, doi: 10.15778/RESIF.YV2011.

Crawford, W. C., and S. C Webb (2000). Identifying and removing Tilt noise from low-frequency (< 0.1 Hz) seafloor vertical seismic data, *Bull. Seismol. Soc. Am.* **90,** no. 4, 952–963, doi: 10.1785/0119990121.

Dewangan, P. R., K. A. Reddy, P. Kamesh Raju, K. K. Singha, V. Aswini, K. Yatheesh, Samudrala, and M. Shuhail (2017). Nature of the ambient noise, site response, and orientation of ocean-bottom seismometers (OBSs): Scientific results of a passive seismic experiment in the Andaman sea, *Bull. Seismol. Soc. Am.* doi: 10.1785/0120170163.

Doran, A. K., and G. Laske (2017). Ocean-bottom seismometer instrument orientations via automated Rayleigh-wave arrival-angle measurements, *Bull. Seismol. Soc. Am.* **107,** no. 2, doi: 10.1785/0120160165.

Dziewoński, A. M., and D. L. Anderson (1981). Preliminary reference Earth model, *Phys. Earth Planet. In.* **25,** no. 4, 297–356, doi: 10.1016/0031-9201(81)90046-7.

16 Geissler, W. H., and R. Schmidt (2013). Short cruise report Maria S. Merian; MSM 24 Walvis BayCape Town, *Technical Report*, Leitstelle Deutsche Forschungsschiffe, Hamburg, Germany, available at https://www.ldf.uni-hamburg.de/merian/wochenberichte/wochenberichte-merian/msm22-msm25/msm24-scr.pdf.

Geissler, W. H., L. Matias, D. Stich, F. Carrilho, W. Jokat, S. Monna, A. Ibenbrahim, F. Mancilla, M. a. Gutscher, V. Sallars, and N. Zitellini (2010). Focal mechanisms for sub-crustal earthquakes in the Gulf of Cadiz from a dense OBS deployment, *Geophys. Res. Lett.* **37,** no. 18, 7–12, doi: 10.1029/2010GL044289.

17 GEOFON Data Centre(1993). *GEOFON Seismic Network*, available at http://dx.doi.org/10.14470/TR560404.

Griffin, O. M. (1985). Vortex-induced vibrations of marine cables and structures, *Technical Report*, Naval Research Lab, Washington, D. C., available at http://www.dtic.mil/docs/citations/ADA157481.

18 Holcomb, G. L. (1989). A direct method for calculating instrument noise levels in side-by-side seismometer evaluations, *Technical Report*, Geological Survey (U.S.), Albuquerque, New Mexico, available at https://pubs.er.usgs.gov/publication/ofr89214.

Hunter, J. D. (2007). Matplotlib: A 2D graphics environment, *Comput. Sci. Eng.* **9,** no. 3, 90–95.

Krischer, L., T. Megies, R. Barsch, M. Beyreuther, T. Lecocq, C. Caudron, and J. Wassermann (2015). ObsPy: A bridge for seismology into the scientific Python ecosystem, *Comput. Sci. Discov.* **8,** no. 1, 014003, doi: 10.1088/1749-4699/8/1/014003.

19 Krüger, S. (2000). Basic shipboard instrumentation and fixed automatic stations for monitoring in the Baltic Sea, in *The Ocean Engineering Handbook*, F. El-Hawary (Editor), CRC Press, 52–61.

Lemke, W., A. Kuijpers, G. Hoffmann, D. Milkert, and R. Atzler (1994). The Darss Sill, hydrographic threshold in the southwestern Baltic: Late Quaternary geology and recent sediment dynamics, *Cont. Shelf Res.* **14,** nos. 7/8, 847–870, doi: 10.1016/0278-4343(94)90076-0.

McNamara, D. E., and R. Buland (2004). Ambient noise levels in the continental United States, *Bull. Seismol. Soc. Am.* **94,** no. 4, 1517–1527, doi: 10.1785/012003001.

Meier, T., W. Friederich, C. Papazachos, T. Taymaz, and R. Kind (2007). EGELADOS: A temporary amphibian broadband seismic network in the southern Aegean, *Geophys. Res. Abstr.* **9,** 9020.

Mohrholz, V., M. Naumann, G. Nausch, S. Krüger, and U. Gräwe (2015). Fresh oxygen for the Baltic Sea—An exceptional saline inflow after a decade of stagnation, *J. Mar. Syst.* **148,** 152–166, doi: 10.1016/j.jmarsys.2015.03.005.

Nissen-Meyer, T., M. van Driel, S. C. Stähler, K. Hosseini, S. Hempel, L. Auer, A. Colombi, and A. Fournier (2014). AxiSEM: Broadband 3-D seismic wavefields in axisymmetric media, *Solid Earth* **5,** no. 1, 425–445, doi: 10.5194/se-5-425-2014.

Peterson, J. (1993). Observations and modeling of seismic background noise, *Technical Report, Open File Rept. 93-322*, Albuquerque, New Mexico.

Ringler, A. T., and C. R. Hutt (2010). Self-noise models of seismic instruments, *Seismol. Res. Lett.* **81,** no. 6, 972–983, doi: 10.1785/gssrl.81.6.972.

Ringler, A. T., R. Sleeman, C. R. Hutt, and L. S. Gee (2014). Seismometer self-noise and measuring methods, in *Encyclopedia of Earthquake Engineering*, 1–13, Springer Berlin Heidelberg, Heidelberg, Germany, doi: 10.1007/978-3-642-36197-5_175-1.

Ryberg, T., W. H. Geissler, W. Jokat, and S. Pandey (2017). Uppermost mantle and crustal structure at Tristan da Cunha derived from ambient seismic noise, *Earth Planet. Sci. Lett.* **471,** 117–124, doi: 10.1016/j.epsl.2017.04.049.

Skop, R. A., and O. M. Griffin (1975). On a theory for the vortex-excited oscillations of flexible cylindrical structures, *J. Sound Vib.* **41,** no. 3, 263–274, doi: 10.1016/S0022-460X(75)80173-8.

Snelling, B. (2015). *T*-waves and Tectonics: A survey of acoustic signals generated by tectonic processes on spreading ridges in the Indian Ocean, *Master Thesis*, University of Oxford, Oxford, United Kingdom.

Stähler, S. C., K. Sigloch, G. Barruol, W. C. Crawford, K. Hosseini, and 20
M. C. Schmidt-Aursch (2015). Revised noise levels at all stations of the RHUM-RUM ocean-bottom-seismometer network, *Technical Report*.

Stähler, S. C., K. Sigloch, K. Hosseini, W. C. Crawford, G. Barruol, M. C. Schmidt-Aursch, M. Tsekhmistrenko, J.-R. Scholz, A Mazzullo, and M. Deen (2016). Performance report of the RHUM-RUM ocean bottom seismometer network around La Réunion, western Indian Ocean, *Adv. Geosci.* **41,** 43–63, doi: 10.5194/adgeo-41-43-2016.

Tasič, I., and F. Runovc (2012) Seismometer self-noise estimation using a single reference instrument, *J. Seismol.* **16,** no. 2, 183–194, doi: 10.1007/s10950-011-9257-4.

Triantafyllou, M. S., R. Bourguet, J. Dahl, and Y. Modarres-Sadeghi (2016). Vortex-induced vibrations, in *Springer Handbook Ocean Engineering*, Springer International Publishing, Cham, Switzerland, 819–850, doi: 10.1007/978-3-319-16649-0_36..

Van Driel, M., L. Krischer, S. C. Stähler, K. Hosseini, and T. Nissen-Meyer (2015). Instaseis: Instant global seismograms based on a broadband waveform database, *Solid Earth* **6,** no. 2, 701–717, doi: 10.5194/se-6-701-2015.

Webb, S. C. (1998). Broadband seismology and noise under the ocean, *Rev. Geophys.* **36,** no. 1, 105–142, doi: 10.1029/97RG02287.

Simon C. Stähler
Institute of Geophysics, ETH Zürich
Sonneggstrasse 5
8092 Zurich, Switzerland
simon.staehler@erdw.ethz.ch

Mechita C. Schmidt-Aursch
Alfred Wegener Institute

Helmholtz Centre for Polar and Marine Research
Am Alten Hafen 26
27568 Bremerhaven, Germany
Mechita. Schmidt-Aursch@awi.de

Gerrit Hein
Institute of Geophysics
University of Hamburg
Bundesstrasse 55
20146 Hamburg, Germany
Gerrit. Hein@studium.uni-hamburg.de

Robert Mars
Leibniz Institute for Baltic Sea Research (IOW)
Seestrasse 15
18119 Rostock, Germany
robert.mars@io-warnemuende.de

QUERIES

1. AU: Please provide a definition of “LOBSTER”; it will be included before the abbreviation.
2. AU: Please provide a definition of “AWI”; it will be included before the abbreviation.
3. AU: Please provide a definition of “RHUM-RUM”; it will be included before the abbreviation.
4. Au: Tilt OK here?
5. AU: Please provide a definition of “ROV”; it will be included before the abbreviation.
6. AU: Does the asterisk represent (1) multiplication (so would be replaced by a multiplication sign or closed up, whichever you prefer), (2) convolution in cross correlation (in which the asterisk would be centered), or (3) a complex conjugate of a complex number (in which the asterisk would be set as a superscript)?
7. AU: Does the centered dot represent (1) multiplication (so would be replaced by a multiplication sign, closed up, or information placed in parentheses) or (2) a dot product (in which the dot will be left in the equation)? If option (1) is correct, please either indicate you wish the multiplication symbol to be used *or* provide a revised equation with correctly located parentheses as needed for clarity of mathematical groupings. If option (2) is correct, please provide revised wording that indicates the dot product is intended in the equation.
8. AU: Please provide a definition of “AxiSEM”; it will be included before the abbreviation.
9. AU: Please provide a definition of “PREM”; it will be included before the abbreviation.
10. AU: Please indicate if the roman capital M throughout the article should be changed to (1) bold **M** or (2) Mw (italic “M” and subscript roman “w”).
11. AU: Please provide the month and year when you last accessed the websites in this section for your article.
12. AU: Please provide a definition of “RESIF”; it will be included before the abbreviation.
13. AU: Please provide the month and year when you last accessed this website (http://www.kum-kiel.de) for your article.
14. AU: Please note the DOI for Alfred-Wegener-Institut Helmholtz-Zentrum für Polar- und Meeresforschung *et al.* (2017), as written, does not appear in the DOI system. Please check the DOI number and provide corrections.
15. AU: Hyphen OK here after Polar?
16. AU: Please provide the month and year when you last accessed this website for your article.
17. AU: Please provide the month and year when you last accessed this website for your article.
18. AU: Please provide the month and year when you last accessed this website for your article.
19. AU: Please provide publisher location (city and country) for this reference.
20. AU: Please provide report number or any additional information available for this reference.
21. AU: Please provide significance for "?" if any to include in the caption.
22. AU: Because the figures will only appear in color online, and the text will be the same both online and in print, references to specific colors must be removed throughout the figure captions. Please provide revised wording and/or revised figures as needed.
23. AU: Please provide the section title you intended here in place of "text" for the cross-reference. (SSA will include hyperlinks to cross-references in the electronic edition to help the reader navigate through the document.)
24. AU: Because the figures will only appear in color online, and the text will be the same both online and in print, references to specific colors must be removed throughout the figure captions. Please provide revised wording and/or revised figures as needed.